Journal of Computational and Applied Mathematics 422 (2023) 114891

Contents lists available at ScienceDirect

Journal of Computational and Applied Mathematics

journal homepage: www.elsevier.com/locate/cam

Pricing renewable energy certificates with a Crank–Nicolson Lagrange–Galerkin numerical method

María A. Baamonde-Seoane, María-del-Carmen Calvo-Garrido, Carlos Vázquez *

Department of Mathematics, Faculty of Informatics, University A Coruña and CITIC, Campus de Elviña s/n 15071 A Coruña, Spain

ARTICLE INFO

Article history:
Received 2 November 2021
Received in revised form 3 October 2022

Keywords:
Renewable energy certificates
Green certificates
Nonlinear PDE
Crank–Nicolson
Lagrange–Galerkin method
Maximal monotone operator

ABSTRACT

The valuation problem of renewable energy certificates can be formulated in terms of a nonlinear PDE model where the underlying stochastic factors are the accumulated green certificates sold by an authorized producer and the natural logarithm of the renewable generation rate. In the present paper, the nonlinear convective term is treated with the Bermúdez–Moreno duality method for maximal monotone operators as in Baamonde-Seoane et al. (2021). The main novelty of this article comes from the proposed techniques for the numerical solution of the resulting linear problem. In this case, we propose a Lagrange–Galerkin method which mainly consists of Crank–Nicolson characteristics for time discretization combined with finite elements for the discretization in the accumulated green certificates and the natural logarithm of the renewable generation rate directions. Finally, several numerical examples are presented to illustrate the good performance of the method and model, and its comparison with other numerical schemes employed to solve the same problem.

1. Introduction

Climate change has emerged as one of the most important global issues of the 21st century. The growth of greenhouse gases concentrations in the atmosphere are responsible for the anthropogenic greenhouse effect, with an increase in the average air surface temperature. This change has several impacts on the environment, such as the appearance of extreme weather events. In recent years, governments around the world have implemented different policies to reduce greenhouse gas emissions and encourage the growth of renewable energy usage. The most well known of these policies are the cap-and-trade markets.

In cap-and-trade markets, the market is subject to an Emissions Trading Scheme (ETS) in which regulators impose a limit to carbon emissions (cap) during one compliance period. Each registered firm receives an initial allocation of allowances in the amount of this limit, each one allowing for a unit of CO_2 emission, usually one tonne. These allowances can be used to offset its cumulative emissions at the end of the compliance period. If a firm produces a higher level of emissions than its owned allowances permit, then the firm must pay a penalty per extra tonne of CO_2 emitted. Throughout a compliance period, allowances are actively traded and this leads to the formation of a price, which represents the cost of carbon. This is the trade part of a cap-and-trade scheme. The behaviour of prices in ETS has already attracted considerable

* Corresponding author.
E-mail addresses: maria.baamonde1@udc.es (M.A. Baamonde-Seoane), carmen.calvo.garrido@udc.es (M.C. Calvo-Garrido), carlosv@udc.es (C. Vázquez).

https://doi.org/10.1016/j.cam.2022.114891

interest in the literature (see [1–3]). In practice, an ETS has multiple compliance periods, each one with its own distinct cap and penalty. Between these periods, an ETS can provide some flexibility for firms to reduce emissions.

Renewables are considered by many policy-makers to contribute to improving energy security and protecting the environment. On an average cost basis, some renewables in the best locations are competitive with conventional energy sources. However, in many cases renewables are not competitive yet. Supportive policies are still needed to encourage the further development and deployment especially of "new" renewables in energy markets.

Nowadays, several governments have developed environmental policies in order to encourage renewable energy sources and promote targets for renewable energy production. As it is also mentioned in [4], many countries or states have adopted Renewable Portfolio Standards (RPSs) and trading of Renewable Energy Certificates (RECs). Through these schemes, electric utility quote obligations are supported and a certain percentage of the electricity from renewable energy sources is required. This required percentage is generally increased annually by a regulator to meet longer-term policy targets.

However, renewable energy technologies often require a huge investment, hence it is necessary to have alternative market tools to get the required targets. An interesting and closely related alternative is the markets for tradable RECs, which can be used to encourage the growth of a particular type of renewable energy, as in the case of Solar Renewable Energy Certificates (SRECs) (see [5,6]). A REC (or green certificate) is a financial instrument traded in the marketplace, which guaranties that an amount of electricity has been produced by means of renewable energy sources such as solar or wind plants, for example. One certificate is issued to the renewable power generator for each MWh or higher units of energy produced. Thus, tradable green certificates are designed to promote electricity generation from renewable energy sources.

On one hand, this kind of contracts are used by companies (buyers) to cover their requirements of supplying "clean" electricity by purchasing green certificates instead of making a huge investment in technologies to produce renewable energy themselves. In [7], the optimal percentage requirement of the total electricity production that must be obtained from renewable sources is analysed. On the other hand, sellers can fund the cost of renewable energy installations by selling the certificates.

There are similarities between REC markets and carbon cap-and-trade ones, however there are also some differences. The main important difference comes from the uncertainty in the market. In the former market, it is the supply of certificates (driven by some generation process), while in the latter, it is the demand for allowances (driven by an emission process). Furthermore, the regulator now fixes demand (requirement) instead of supply (cap), and borrowing and withdrawal are not present.

Due to the necessity of fighting against climate change, in the last years the production of electricity from energy renewable sources has increased and consequently the demand of this kind of certificates has grown. RECs markets can provide opportunities for investing, although the risk due to their volatile price behaviour is significant. Therefore, the study of these markets and their characteristics have begun to gain attraction.

There are several references discussing tradable green certificates in different world regions. In [8], the tradable green certificates system in some regions of Belgium is studied and the particular system established in the Flemish region is analysed in detail. More recently, the effects of the new Chinese government policy about green certificates pricing and transaction decisions are evaluated in [9] and [10].

In the literature, the valuation problem of green certificates has been tackled with different models and techniques. In [11], for the particular case of the Swedish–Norwegian market, the valuation problem is modelled as a control problem for which the authors derive a closed formula. In [12], the authors describe three models based on game theory approach for the implementation of the tradable green certificates system. The valuation of solar renewable energy certificates in the New Jersey market is treated in the Ref. [5], where the price of the SREC is achieved by using a dynamic programming algorithm. Moreover, the renewable energy production rate is modelled by means of a geometric Brownian motion process instead of the Ornstein–Uhlenbeck (OU) process considered in the present work.

From the mathematical point of view, the valuation problem of green certificates can also be modelled as a PDE problem associated with a nonlinear operator. In previous works existing in the literature, nonlinear PDEs also appear in the valuation of financial instruments in emission markets with the possibility of multiple periods for which an obligation is set. For example, in [1] the authors describe the asymptotic behaviour of the solution close to the end of a compliance period.

In the present paper, assuming that the price of the certificate depends on two stochastic factors which are the accumulated green certificates and the renewable energy production rate, we present the PDE model that governs the valuation of such financial instruments and we propose appropriate numerical methods for its solution. It is important to highlight that although the PDE model and the treatment of the nonlinear convective term are also presented in our previous work [4], the numerical techniques applied to solve the problem are different.

In the literature, the same stochastic factors are considered in [11]. Nevertheless, the formulation of the problem and the numerical techniques are different as well.

For the numerical solution of the nonlinear PDE problem, we first apply the Bermúdez–Moreno algorithm proposed in [13] to deal with the nonlinear convective term. This duality method is based on the approximation of a nonlinear maximal monotone operator by means of its Yosida regularization. Next, the resulting linear problem is discretized by using a Lagrange–Galerkin method which mainly consists of Crank–Nicolson characteristics scheme for time discretization

combined with finite elements for the discretization in the accumulated green certificates and the natural logarithm of the renewable generation rate directions, which is the main contribution of this paper. These numerical techniques, which result very efficient for convection dominated problems as the one treated in this work, were developed in [14] for Asian option pricing problems. Moreover, in [15] the authors address the numerical analysis of the here proposed characteristics Crank–Nicolson time discretization method for a wide class of convection–diffusion–reaction PDE problems. Additionally, the fully discretized problem obtained by the combination of Crank–Nicolson characteristics with Lagrange finite elements is studied in [16].

In the previous paper [4], the same PDE model is posed to price a REC and the same duality method for the nonlinear term are used. However, in [4] the resulting linear problem is solved by a semi-Lagrangian scheme in the direction without diffusion while an implicit second order finite differences scheme is applied in the direction with diffusion term. In the present paper, we show the differences with respect to this previous work and the relevant improvements obtained in the computational when applying the numerical schemes here proposed.

The organization of the paper is as follows. In Section 2, the mathematical modelling for pricing renewable energy certificates is posed. We introduce the stochastic processes which describe the evolution of the number of accumulated green certificates and the natural logarithm of the renewable generation rate. In Section 3, we formulate the PDE problem which governs the valuation of RECs. In Section 4, we describe the proposed numerical techniques to obtain a solution of the PDE problem. Section 5 presents some examples in order to illustrate the performance of the proposed models and numerical methods. Finally, Section 6 contains some conclusions.

2. Mathematical model for the valuation of renewable energy certificates

In this section we introduce the mathematical modelling when considering two stochastic factors. In what follows, for a fixed time horizon representing the end of the compliance period $T > 0$, we assume that the source of randomness in the model is given by one-dimensional Wiener process $W = (W_t)_{0\leq t\leq T}$. We assume that this Wiener process is defined on a complete probability space $(\Omega, \mathcal{F}, \mathbb{P})$, and it is adapted to the filtration $\mathbb{F} = \{\mathcal{F}_t,\ t \geq 0\}$.

Assuming that the price of a green certificate depends on two stochastic factors, which are the renewable generation rate, G_t, and the number of accumulated green certificates, B_t, we aim to address the model for pricing a REC. For this purpose, we will start describing the stochastic processes that govern the dynamics of both factors.

First, let us denote by $\tilde{G}_t = \ln(G_t)$ the Ornstein–Uhlenbeck (OU) process, which satisfies the following stochastic differential equation (SDE):

$$d\tilde{G}_t = \gamma_g \left(\xi(t) + \frac{\delta_g}{\gamma_g} P_t - \tilde{G}_t \right) dt + \sigma_g dW_t, \tag{1}$$

assuming that $G_{t_0} = g_0$, and where γ_g is the mean reversion speed of the process, P_t is the certificate price, δ_g is the parameter which controls the level of immediate feedback from the price of the certificate, σ_g is the volatility and W_t is the Wiener process governing the stochastic part of the equation. Moreover, taking into account that weather conditions strongly affect the production of energy in the renewable power generation, we introduce a deterministic function $\xi(t)$ representing the seasonality effect. Seasonal patterns exist in most markets and this approach is now present in virtually all models. It was in [17] the first time that a deterministic or seasonal component was incorporated into a spot price model. A common choice is to use a combination of trigonometric functions as it is proposed in [5]. Nevertheless, there are other possibilities such as the one considered in [11], which consists on using time series models to describe statistical features of weather factors. Furthermore, in the OU process (1), the mean reversion level is linear in P_t plus seasonality. Now, having in view the previous stochastic process, the production of renewable energy G_t can be written as

$$G_t = \exp\left(\tilde{G}_t\right).$$

Secondly, we introduce de dynamics of the number of accumulated renewable energy certificates, B_t,

$$dB_t = G_t dt.$$

Note that B_t is non-negative and non-decreasing because it represents an accumulated quantity, and we assume that $B_{t_0} = 0$, where t_0 is the beginning of the compliance period.

3. Statement of the pricing PDE

If we denote by $P = P(t, \tilde{G}, B)$ the price of the renewable energy certificate at time t, by using a dynamic hedging technique in a similar way to the valuation problem of swing options (see [18], for more details) and applying Itô's Lemma (see [19]), we can derive the following nonlinear PDE whose solution is the price of the REC:

$$\mathcal{L}[P] = \frac{\partial P}{\partial t} + \frac{1}{2}\sigma_g^2 \frac{\partial^2 P}{\partial \tilde{G}^2} + \gamma_g \left(\xi(t) - \tilde{G} \right) \frac{\partial P}{\partial \tilde{G}} + \delta_g P \frac{\partial P}{\partial \tilde{G}} + \exp(\tilde{G}) \frac{\partial P}{\partial B} - rP = 0, \tag{2}$$

where r is the constant risk free interest rate.

Assuming that the number of life years of the certificate is denoted by y and the maturity of the certificate is T, the PDE problem associated to (2) is initially formulated in the unbounded domain $(T-y, T)\times(-\infty, \infty)\times(0, \infty)$. Note that the PDE operator (2) has a nonlinear convective term adding an extra difficulty to the problem.

For the particular case of one single period (i.e. one year, $y = 1$), the payoff at the expiry date of the certificate, T, is a decreasing function in the number of accumulated green certificates at maturity, B, and depends on the requirement on the percentage of energy obtained from renewables at maturity, R_T. Thus, in order to state the PDE problem, Eq. (2) is completed with the final condition

$$P(T, \tilde{G}, B) = \pi_T \mathbb{1}_{\{B<R_T\}}, \tag{3}$$

where π_T is the penalty amount π at time T. At maturity, the price of the certificate is equal to the penalization if the banked certificates do not meet the requirement, otherwise the price is zero.

Moreover, there exists the possibility of extending the problem to multiple periods. In that case, at each compliance date, T^i, for $i = 1, \ldots, y-1$, a jump condition must be applied. Thus, when the obligation is set the value of the certificate is given by

$$P(T^i, \tilde{G}, B) = \max\left(\pi_{T^i}\mathbb{1}_{\{B<R_i\}}, P\left(T^i_+, \tilde{G}, \max(0, B-R_i)\right)\right). \tag{4}$$

Note that T^i corresponds to the end of the ith life year of the certificate and R_i is the requirement at that time. Thus, Eqs. (2) and conditions (4) establish a sequence of linked final value problems that must be solved from time T to time t_0 with a kind of pasting conditions at the compliance dates T^i.

The study of the existence and uniqueness of solution for the nonlinear PDE problems defined by (2)–(3) or by (2)–(4) remains as an open problem as it is mentioned in [4]. We note that the PDE (2) is non-linear and exhibits some similarities to the one appearing in emission markets in [1], the existence and uniqueness of solution of which is rigorously analysed in [20]. However, the ideas in [20] cannot be employed to analyse the existence and uniqueness of solution of (2). The main reason is that in [20], the PDE appearing in emission markets is obtained from a FBSDE containing a first forward SDE which is uncoupled with the other two, so that the existence and uniqueness for this first equation can be obtained in a first step. Then, the two remaining equations are understood as SDEs with stochastic drift terms and the methodologies developed in [21–23] can be used.

However, in the here treated problem, the PDE (2) is obtained from a FBSDE with three equations that are coupled each other (see [4]). This is the reason why the existence and uniqueness of solution for PDE problem (2)–(3) remains as an open research line, as well as the same results for the PDE problem (2)–(4).

4. Numerical techniques

In this section we propose a set of numerical techniques to approximate the solution of PDE problems (2)–(2) and (3)–(4) that have been posed in the previous section.

4.1. The duality algorithm

As the drift term depends linearly on the unknown P, the corresponding first order (convective) term in the PDE (2) introduces a nonlinear aspect that needs to be solved. More precisely, the governing PDE is semilinear. A possible approach could be to treat this nonlinear term in a semi-explicit way in the time discretization, by considering the drift coefficient evaluated at the previous time step, which linearizes the problem to be solved at each time step. However, implicit methods are usually preferred to explicit or semi-explicit ones. As in [4], the Bermúdez–Moreno algorithm proposed in [13] will be applied. This algorithm is a duality method, which is based on the approximation of nonlinear monotone operators by means of its Yosida regularization. It was previously applied to the simulation of read/write processes in magnetic storage devices in [24] for the treatment of a nonlinear diffusive term in the PDE operator instead of a nonlinear convection term. Furthermore, in [25] the convergence of the method in the nonlinear diffusion setting has been analysed. Next, in [26] the methodology has been extended from one to two spatial variables.

Thus, as in [4], we define the maximal monotone operator

$$h(P) = \begin{cases} P^2 & \text{if } P \geq 0 \\ 0 & \text{if } P < 0 \end{cases}, \tag{5}$$

so that Eq. (2) can be written in the form:

$$\frac{\partial P}{\partial t} + \frac{1}{2}\sigma_g^2\frac{\partial^2 P}{\partial \tilde{G}^2} + \gamma_g\left(\xi(t) - \tilde{G}\right)\frac{\partial P}{\partial \tilde{G}} + \frac{\delta_g}{2}\frac{\partial h(P)}{\partial \tilde{G}} + \exp(\tilde{G})\frac{\partial P}{\partial B} - rP = 0. \tag{6}$$

Next, we consider a parameter $\omega > 0$ and introduce the additional unknown $\theta = h(P) - \omega P = (h - \omega I)(P)$, so that

$$h(P) = \theta + \omega P \tag{7}$$

and

$$\frac{\partial h(P)}{\partial \tilde{G}} = \frac{\partial \theta}{\partial \tilde{G}} + \omega \frac{\partial P}{\partial \tilde{G}}. \tag{8}$$

Now, following the results in [13], we have

$$\theta = h_\lambda^\omega(P + \lambda\theta) \tag{9}$$

where h_λ^ω is the Yosida approximation of the operator $h_\omega = h - \omega I$ with parameter λ, which is given by $h_\lambda^\omega = (I - K_\lambda^\omega)/\lambda$, where $K_\lambda^\omega = (I + \lambda_\omega)^{-1}$ is the resolvent operator of h_ω with parameter λ, which is defined for $\lambda\omega < 1$ and it is a monotone Lipschitz function with constant $(1-\lambda\omega)^{-1}$, see [27] for details about maximal monotone operators and Yosida approximation.

As indicated in [4], the choice $\lambda = 1/2\omega$ has been proved to be optimal in several application and in some particular cases supported by theoretical results, thus obtaining the following expression for the Yosida approximation:

$$h_{1/2\omega}^\omega\left(P + \frac{\theta}{2\omega}\right) = \begin{cases} -\theta - 2\omega P & \text{if } P + \frac{\theta}{2\omega} < 0 \\ \theta + 2\omega P + \omega^2 - \omega\sqrt{4\theta + 8\omega P + \omega^2} & \text{if } P + \frac{\theta}{2\omega} \geq 0 \end{cases}. \tag{10}$$

As pointed out in [24], the convergence of Bermúdez–Moreno algorithm depends on the parameter ω which, in turn, depends on the exact solution.

Next, using (7)–(8), the PDE (6) can be replaced by

$$\frac{\partial P}{\partial t} + \frac{1}{2}\sigma_g^2 \frac{\partial^2 P}{\partial \tilde{G}^2} + \gamma_g\left(\xi(t) - \tilde{G}\right)\frac{\partial P}{\partial \tilde{G}} + \frac{\delta_g \omega}{2}\frac{\partial P}{\partial \tilde{G}} + \exp(\tilde{G})\frac{\partial P}{\partial B} - rP = -\frac{\delta_g}{2}\frac{\partial \theta}{\partial \tilde{G}}. \tag{11}$$

Note that PDE (11) is coupled with the nonlinear equation (9). Moreover, for a given θ, PDE (11) is linear. Thus, the idea of Bermúdez–Moreno algorithm we propose mainly consists of a fixed point iteration between the numerical solution of PDE (11) and Eq. (9) at each time step, as will be explained in the forthcoming section.

4.2. Formulation of the PDE problem in a bounded domain

In order to apply numerical techniques to solve the linear PDE problem (11) for a given value of θ, it is first necessary to truncate the initial unbounded spatial domain to a bounded one and to impose boundary conditions where they are required. For this purpose, let $\bar{G}_\infty$ and B_∞ be appropriately chosen real numbers large enough so that the truncation of the domain does not affect the solution of the problem in the region of interest. The choice of the values to truncate the domain depends on the requirement which is involved in the payoff function and in the jump conditions at compliance dates. Once the truncation values are chosen, we consider the spatial bounded domain $(-\tilde{G}_\infty, \tilde{G}_\infty)\times(0, B_\infty)$ and introduce the following change of spatial variables:

$$a_1 = \frac{\tilde{G} + \tilde{G}_\infty}{\bar{G}_\infty},\ a_2 = \frac{B}{B_\infty},$$

where $\bar{G}_\infty = 2\tilde{G}_\infty$. Thus, with the previous change of variables we transform the bounded spatial domain $(-\tilde{G}_\infty, \tilde{G}_\infty) \times (0, B_\infty)$ into the domain $\Omega = (0, 1) \times (0, 1)$, whose boundary can be decomposed as $\Gamma = \bigcup_{i=1}^2(\Gamma_i^- \cup \Gamma_i^+)$ where

$$\Gamma_i^- = \{(a_1, a_2) \in \Gamma |\ a_i = 0\},\ \Gamma_i^+ = \{(a_1, a_2) \in \Gamma |\ a_i = 1\},\ i = 1, 2,$$

Next, as in [4], we follow the methodology introduced by [28] to obtain the boundaries where it is necessary to impose boundary conditions. On those boundaries, we will impose homogeneous Neumann boundary conditions.

Once we have introduced the bounded domain and the boundary conditions, in order to obtain a PDE problem with initial condition, we consider the change of time variable $\tau = T - t$, where τ represents the time to maturity. So, the PDE (11) jointly with final and boundary conditions can be equivalently formulated as the following initial–boundary value problem:

find $P : [0, y] \times \Omega \to \mathbb{R}$ such that

$$\frac{\partial P}{\partial \tau} - Div(\mathcal{A}\nabla P) + \vec{v}\cdot\nabla P + lP = \hat{f} + \frac{\delta_g \bar{G}_\infty}{2}\frac{\partial \theta}{\partial a_1} \text{ in } (0, y) \times \Omega\,, \tag{12}$$

$$P(0, \cdot) = \pi_T \mathbb{1}_{\{a_2 B_\infty < R_T\}} \text{ in } \Omega, \tag{13}$$

$$\frac{\partial P}{\partial a_1} = 0 \text{ on } (0, y) \times (\Gamma_1^- \cup \Gamma_1^+), \tag{14}$$

$$\frac{\partial P}{\partial a_2} = 0 \text{ on } (0, y) \times \Gamma_2^+, \tag{15}$$

jointly with jump conditions (4) at compliance dates.

Moreover, in (12), the diffusion matrix $\mathcal{A}$, the velocity field $\vec{v}$, the linear term l and the second member function $\hat{f}$ have the following expressions:

$$\mathcal{A} = \begin{pmatrix} \frac{1}{2}(\sigma_g \bar{G}_\infty)^2 & 0 \\ 0 & 0 \end{pmatrix},$$
$$\vec{v} = \begin{pmatrix} \left(-\gamma_g \left(\xi(T-\tau) - (a_1 \bar{G}_\infty - \tilde{G}_\infty)\right) - \frac{\delta_g \omega}{2}\right) \bar{G}_\infty \\ -B_\infty \exp(a_1 \bar{G}_\infty - \tilde{G}_\infty) \end{pmatrix},$$
$$l = r,$$
$$\hat{f} = 0.$$

4.3. The Crank Nicolson characteristics method

In order to obtain a time discretization of the problem (12), we propose a Crank–Nicolson characteristic method. This numerical scheme mainly consists of approximating the material derivative along the characteristics curves with a finite differences method. Moreover, in this method, the convective term is treated explicitly leading to a symmetric system of equations.

First, let us define

$$\frac{DP}{D\tau} = \frac{\partial P}{\partial \tau} + \vec{v} \cdot \nabla P,$$

which represents the material derivative along the characteristic curve through $a = (a_1, a_2)$ at time $\bar{s}$, $\chi(a, \bar{s}; s)$, which is the solution of the following final value ODE problem:

$$\frac{\partial}{\partial s}\chi(a, \bar{s}; s) = \vec{v}(\chi(a, \bar{s}; s), s), \quad \chi(a, \bar{s}; \bar{s}) = a. \tag{16}$$

In order to discretize in time the material derivative, we introduce a number of time steps $N_T > 0$, a time step $\Delta\tau = y/N_T$ and the time mesh points $\tau^n = n\Delta\tau$, $n = 0, \frac{1}{2}, 1, \frac{3}{2}, \ldots, N_T$.

Now, we approximate the material derivative at time $\tau^{n+\frac{1}{2}}$ by the quotient:

$$\frac{DP}{D\tau} \approx \frac{P^{n+1} - P^n \circ \chi^n}{\Delta\tau},$$

where $\chi^n(a) = \chi(a, \tau^{n+1}; \tau^n)$.

In some cases, the expressions of the characteristics curves can be obtain analytically. For example, when the seasonality function ξ is equal to zero the components of $\chi^n(a)$ are given by

$$\chi_1^n(a) = \left(-\gamma_g(a_1 \bar{G}_\infty - \tilde{G}_\infty) + \frac{\delta_g \omega}{2}\right) \bar{G}_\infty \Delta\tau + a_1,$$
$$\chi_2^n(a) = B_\infty \Delta\tau \exp(a_1 \bar{G}_\infty - \tilde{G}_\infty) + a_2.$$

However, sometimes it is necessary to approximate the characteristics by using numerical ODE solvers. In this work we will implement a second order explicit Runge–Kutta scheme for the cases in which the computation of an analytical solution of the final value problem (16) is not possible.

Now, let us write the Crank–Nicolson characteristics time discretization around $(\chi(a, \tau^{n+1}; \tau^{n+\frac{1}{2}}), \tau^{n+\frac{1}{2}})$, $n = 0, \ldots, N_T - 1$, for the first equation of (12), namely:

$$\begin{aligned} \frac{P^{n+1}(a) - P^n(\chi^n(a))}{\Delta\tau} - \frac{1}{2}Div(\mathcal{A}\nabla P^{n+1})(a) - \frac{1}{2}Div(\mathcal{A}\nabla P^n)(\chi^n(a)) \\ + \frac{1}{2}(lP^{n+1})(a) + \frac{1}{2}(lP^n)(\chi^n(a)) = \frac{1}{2}\hat{f}^{n+1}(a) + \frac{1}{2}\hat{f}^n(\chi^n(a)) \\ + \frac{1}{2}\frac{\delta_g \bar{G}_\infty}{2}\left(\frac{\partial \theta^{n+1}}{\partial a_1}(a) + \frac{\partial \theta^n}{\partial a_1}(\chi^n(a))\right). \end{aligned} \tag{17}$$

Moreover, at each time step, Eq. (17) is coupled with the following nonlinear relation between P^{n+1} and θ^{n+1};

$$\theta^{n+1} = h^\omega_{1/2\omega}\left(P^{n+1} + \frac{1}{2\omega}\theta^{n+1}\right). \tag{18}$$

4.4. Fixed point algorithm

In order to approximate the solution of the nonlinear problem (17)–(18) at each iteration of the characteristics method, we propose the following fixed point scheme:

(1) Let $N_T > 0$, $\epsilon > 0$, P^0, θ^0 given.
(2) For $n = 0, 1, 2, \ldots, N_T - 1$

A. Let $\theta^{n+1,0} = \theta^n$.
B. For $k = 0, 1, 2, \ldots$

- For $\theta^{n+1,k}$ known, we obtain $P^{n+1,k+1}$ solving the linear problem

$$\begin{aligned}\frac{P^{n+1,k+1}(a) - P^n(\chi^n(a))}{\Delta\tau} - \frac{1}{2}Div(\mathcal{A}\nabla P^{n+1,k+1})(a)\\ -\frac{1}{2}Div(\mathcal{A}\nabla P^n)(\chi^n(a)) + \frac{1}{2}(lP^{n+1,k+1})(a)\\ +\frac{1}{2}(lP^n)(\chi^n(a)) = \frac{1}{2}\hat{f}^{n+1}(a) + \frac{1}{2}\hat{f}^n(\chi^n(a))\\ +\frac{1}{2}\frac{\delta_g\bar{G}_\infty}{2}\left(\frac{\partial\theta^{n+1,k}}{\partial a_1}(a) + \frac{\partial\theta^n}{\partial a_1}(\chi^n(a))\right),\end{aligned} \tag{19}$$

  jointly with the boundary conditions.
- We set

$$\theta^{n+1,k+1} = h^{\omega}_{1/2\omega}\left(P^{n+1,k+1} + \frac{1}{2\omega}\theta^{n+1,k}\right)$$

- We check the stopping test

$$\frac{\|\theta^{n+1,k+1} - \theta^{n+1,k}\|_\infty}{\|\theta^{n+1,k+1}\|_\infty} < \epsilon.$$

C. We go to 2 if the stopping condition is met, otherwise we repeat the above steps starting at B.

4.5. Spatial discretization

For the spatial discretization of the linear problem (19), we propose biquadratic Lagrange finite elements. Thus, first, we need to obtain a variational formulation of such problem at each time step $n = 0, 1, 2, \ldots, N_T - 1$, and each fixed point iteration, $k = 0, 1, 2, \ldots$. For this purpose, we multiply (19) by a suitable test function, $\phi \in H^1(\Omega)$ and we integrate in Ω.

Moreover, assuming that $\chi^n \in \mathcal{C}^2(\Omega)$ and $(\nabla\chi^n)^{-1} \in \mathcal{C}^1(\Omega)$, we apply Green's theorems, such as the classical Green formula and the following one proposed in [29]:

$$\begin{aligned}\int_\Omega Div(\mathcal{A}\nabla P^n)(\chi^n(a))\phi(a)\,da = &\int_\Gamma (\nabla\chi^n)^{-T}(a)\vec{n}(a)\cdot(\mathcal{A}\nabla P^n)(\chi^n(a))\phi(a)\,dA\\ &- \int_\Omega (\nabla\chi^n)^{-1}(a)(\mathcal{A}\nabla P^n)(\chi^n(a))\cdot\nabla\phi(a)\,da\\ &- \int_\Omega Div((\nabla\chi^n)^{-T}(a))\cdot(\mathcal{A}\nabla P^n)(\chi^n(a))\phi(a)\,da,\end{aligned} \tag{20}$$

where $\vec{n}$ is a vector normal to the boundary pointing outward and dA denotes the integration measure on the boundary Γ.

Note that for the particular case in which there is no seasonality effect, i.e. $\xi = 0$, we can obtain the analytical expression of the inverse of the gradient of the characteristics, which is given by:

$$(\nabla\chi^n)^{-1}(a) = \begin{pmatrix} \dfrac{1}{-\gamma_g\Delta\tau(\bar{G}_\infty)^2 + 1} & 0\\ \dfrac{-\bar{G}_\infty B_\infty\Delta\tau\exp(a_1\bar{G}_\infty - \tilde{G}_\infty)}{-\gamma_g\Delta\tau(\bar{G}_\infty)^2 + 1} & 1\end{pmatrix},\ Div((\nabla\chi^n)^{-T}(a)) = 0$$

Taking into account the previous value of tensor $(\nabla\chi^n)^{-1}$, appropriate Green's formulas and having in view that $\vec{n}\cdot\mathcal{A}\nabla P^{n+1} = 0$ on Γ due to the boundary conditions imposed in the problem (12)–(15), we can achieve the following variational formulation for the time discretized problem (19):

find $P^{n+1,k+1} \in H^1(\Omega)$ such that,

$$\begin{aligned}
&\int_\Omega P^{n+1,k+1}(a)\phi(a)\,da + \frac{\Delta\tau}{2}\int_\Omega (\mathcal{A}\nabla P^{n+1,k+1})(a)\cdot\nabla\phi(a)\,da\\
&+ \frac{\Delta\tau}{2}\int_\Omega lP^{n+1,k+1}(a)\phi(a)\,da = \int_\Omega P^n(\chi^n(a))\phi(a)\,da\\
&- \frac{\Delta\tau}{2}\int_\Omega (\nabla\chi^n)^{-1}(a)(\mathcal{A}\nabla P^n)(\chi^n(a))\cdot\nabla\phi(a)\,da - \frac{\Delta\tau}{2}\int_\Omega lP^n(\chi^n(a))\phi(a)\,da\\
&+ \frac{\Delta\tau}{2}\int_\Gamma (\nabla\chi^n)^{-T}(a)\vec{n}(a)\cdot(\mathcal{A}\nabla P^n)(\chi^n(a))\phi(a)\,dA\\
&+ \frac{\Delta\tau}{2}\int_\Omega \hat{f}^{n+1}(a)\phi(a)\,da + \frac{\Delta\tau}{2}\int_\Omega \hat{f}^n(\chi^n(a))\phi(a)\,da\\
&+ \frac{\Delta\tau}{2}\int_\Omega \frac{\delta_g\bar{G}_\infty}{2}\frac{\partial\theta^{n+1,k}}{\partial a_1}(a)\phi(a)\,da + \frac{\Delta\tau}{2}\int_\Omega \frac{\delta_g\bar{G}_\infty}{2}\frac{\partial\theta^n}{\partial a_1}(\chi^n(a))\phi(a)\,da.
\end{aligned} \tag{21}$$

In the general case, when it is not possible to compute the characteristics curves analytically, as it is pointed out in [15], we can employ the following approximations:

$$\begin{aligned}
&(\nabla\chi^n)^{-1}(a) \approx \mathcal{I}(a) + \Delta\tau\mathcal{J}^n(\chi^n(a)) + \mathcal{O}(\Delta\tau^2),\\
&Div((\nabla\chi^n)^{-T}(a)) \approx \Delta\tau\nabla Div(\vec{v}(\chi^n(a))) + \mathcal{O}(\Delta\tau^2).
\end{aligned}$$

where $\mathcal{J}^n = \nabla\vec{v}^n$.

In this work, having in view that $\nabla Div(\vec{v}(\chi^n(a))) = 0$ and considering the previous approximation for the tensor $(\nabla\chi^n)^{-1}(a)$, the weak formulation (21) can be rewritten as

find $P^{n+1,k+1} \in H^1(\Omega)$ such that,

$$\begin{aligned}
&\int_\Omega P^{n+1,k+1}(a)\phi(a)\,da + \frac{\Delta\tau}{2}\int_\Omega (\mathcal{A}\nabla P^{n+1,k+1})(a)\cdot\nabla\phi(a)\,da\\
&+ \frac{\Delta\tau}{2}\int_\Omega lP^{n+1,k+1}(a)\phi(a)\,da = \int_\Omega P^n(\chi^n(a))\phi(a)\,da\\
&+ \frac{\Delta\tau}{2}\int_\Omega (\mathcal{A}\nabla P^n)(\chi^n(a))\nabla\phi(a)\,da - \frac{\Delta\tau}{2}\int_\Omega lP^n(\chi^n(a))\phi(a)\,da\\
&- \frac{\Delta\tau}{2}\int_\Omega \Delta\tau\mathcal{J}^n(\chi^n(a))(\mathcal{A}\nabla P^n)(\chi^n(a))\nabla\phi(a)\,da\\
&+ \frac{\Delta\tau}{2}\int_\Gamma (\mathcal{I}(a) + \Delta\tau\mathcal{J}^n(\chi^n(a)))^T\vec{n}(a)\cdot(\mathcal{A}\nabla P^n)(\chi^n(a))\phi(a)\,dA\\
&+ \frac{\Delta\tau}{2}\int_\Omega \hat{f}^{n+1}(a)\phi(a)\,da + \frac{\Delta\tau}{2}\int_\Omega \hat{f}^n(\chi^n(a))\phi(a)\,da\\
&+ \frac{\Delta\tau}{2}\int_\Omega \frac{\delta_g\bar{G}_\infty}{2}\frac{\partial\theta^{n+1,k}}{\partial a_1}(a)\phi(a)\,da + \frac{\Delta\tau}{2}\int_\Omega \frac{\delta_g\bar{G}_\infty}{2}\frac{\partial\theta^n}{\partial a_1}(\chi^n(a))\phi(a)\,da.
\end{aligned} \tag{22}$$

Now, for the spatial discretization with finite elements, we consider a family of quadrangular meshes $\{\tau_h\}$ of the domain Ω. Associated to each mesh $\{\tau_h\}$, we can introduce a piecewise quadratic Lagrangian finite elements, $(\mathcal{T}, \mathcal{Q}_2, \Sigma_\mathcal{T})$, with $\mathcal{Q}_2$ being the space of polynomials defined in $\mathcal{T} \in \tau_h$ with degree less than or equal to two in each spatial variable, and $\Sigma_\mathcal{T}$ the subset of nodes of the element $\mathcal{T}$. More precisely, we can introduce the finite elements space

$$v_h = \{\psi_h \in \mathcal{C}^0(\Omega) |\ \psi_{h_\mathcal{T}} \in \mathcal{Q}_2, \quad \forall\mathcal{T} \in \tau_h\}, \tag{23}$$

where $\mathcal{C}^0(\Omega)$ is the space of piecewise continuous functions on Ω.

At each step of the proposed duality method, we have to solve numerically the linear PDE (11) by using the formulation (22). Therefore, the numerical analysis of the Lagrange–Galerkin method for solving (11) can be framed in the numerical analysis for the general problem addressed in the two articles [15,16]. In this way, existence and uniqueness of solution for the fully discretized problem of the linear PDE, as well as its convergence, can be obtained. However, we have not addressed the numerical analysis for the coupled problem between the nonlinear equation (9) for the additional unknown θ and the linear PDE (11). The numerical analysis of this coupled formulation for the nonlinear PDE remains as an open problem.

5. Numerical results

In this section we show some numerical examples in order to show the good performance of the numerical techniques and models proposed in the present paper. On one hand, we consider an academic test with an analytical solution in order

Table 1
Number of nodes and elements for quadrangular meshes.

	Mesh 4	Mesh 8	Mesh 16	Mesh 32	Mesh 64
Elements	16	64	256	1024	4096
Nodes	81	289	1089	4225	16641

Table 2
Values for the parameters involved in the PDE model.

Mean reversion speed (γ_g)	2.
Feedback from prices (δ_g)	0.00127
Volatility (σ_g)	0.1863
Interest rate (r)	0.02
Maturity (T)	1.
Years of life (y)	1.

to illustrate the convergence of the numerical methods. On the other hand, as a real case and taking into account the data for Solar Renewable Energy Certificates (SRECs) from the New Jersey market which are provided in [5], we solve the problem (12) to obtain the price of the certificate.

In both examples we have considered the same data as in [4] and we show the numerical results in the same format. This allows the comparison between the set of methods proposed in [4] and the ones presented in this article.

In all the tests, for the finite elements space, we use quadrangular uniform meshes with the number of nodes and elements collected in Table 1.

5.1. Academic test with an analytical solution

As a first numerical example, we consider a test with analytical solution in order to check the numerical method and illustrate its convergence. For this purpose, we compute the second member function u, such that $P(t,\tilde{G},B) = \exp\left((T-t)\tilde{G}B\right)$ is a solution of the nonlinear PDE:

$$\mathcal{L}[P] = u \tag{24}$$

where $\mathcal{L}$ is given by (2) and

$$u(t,\tilde{G},B) = P(t,\tilde{G},B)\times \left[-\tilde{G}B + \frac{1}{2}\sigma_g^2 t^2 B^2 - tB\gamma_g\left(\xi(t) + \frac{\delta_g}{\gamma_g}\exp\left((T-t)\tilde{G}B\right) - \tilde{G}\right) - \exp\left(\tilde{G}\right)t\tilde{G} - r\right].$$

We consider one single period, i.e. one year's life ($y = 1$), $T = 1$ and we pose the PDE problem in the bounded spatial domain $\Omega = (0,1)\times(0,1)$, where the chosen points to truncate the domain are $\tilde{G}_\infty = B_\infty = 1$ in the change of variables.

Moreover, for the duality method we take the parameter $\omega = 2$ and the tolerance $\epsilon = 10^{-5}$. Additionally, the final condition and the boundary conditions on Γ_1^+, Γ_1^- and Γ_2^+ are chosen in agreement with the analytical solution of the PDE. More precisely, we impose Dirichlet boundary conditions with the exact solution on the boundaries where they are required.

In this first test, for the parameters involved in the PDE formulation, we consider the values which are collected in Table 2.

Errors in $L^\infty((0,1);L^2(\Omega))$ discrete norm between the exact and numerical solution, convergence ratio and order are presented in Tables 3 and 4. On one hand, in Table 3 we are assuming that there is not seasonal effect, i.e. $\xi(t) = 0$. In this case the characteristics curves can be computed analytically. On the other hand, in order to compute the errors shown in Table 4, we have taken into account seasonal factors modelled with the following function:

$$\xi(t) = -0.1209\sin(4\pi t) + 0.09\cos(4\pi t) + 0.2151\sin(2\pi t) + 0.3859\cos(4\pi t), \tag{25}$$

which implies that the characteristics curves need to be approximated by using ODE solvers.

Note that the length of the edges of each quadrangular element of the mesh is divided by two when refining the meshes shown in Table 1. Moreover, in both cases, the radius of convergence is given by

$$Ratio = \frac{Error(\tilde{h})}{Error(\frac{\tilde{h}}{2})} \tag{26}$$

where the parameter $\tilde{h}$ indicates that we start with a level of refinement in time and space and we divide by two both, the time and finite element mesh steps to get the results for $\frac{\tilde{h}}{2}$. Thus $Ratio = 2$ corresponds to linear convergence. Finally, the empirical order of convergence is given by $\log_2(Ratio)$.

Table 3
Relative errors in $L^\infty((0,1);L^2(\Omega))$ discrete norm between the exact and numerical solution, convergence ratio and order for the academic test without seasonal effect.

Time steps	Meshes	Error	Ratio	Order
10	Mesh 4	7.9499×10^{-3}	–	–
20	Mesh 8	3.5846×10^{-3}	2.2177	1.1491
40	Mesh 16	1.7029×10^{-3}	2.1049	1.0737
80	Mesh 32	8.4004×10^{-4}	2.0272	1.0195
160	Mesh 64	4.2651×10^{-4}	1.9696	0.9779

Table 4
Relative errors in $L^\infty((0,1);L^2(\Omega))$ discrete norm between the exact and numerical solution, convergence ratio and order for the academic test with seasonal effect.

Time steps	Meshes	Error	Ratio	Order
10	Mesh 4	2.8348×10^{-2}	–	–
20	Mesh 8	1.3784×10^{-2}	2.0565	1.0402
40	Mesh 16	6.7905×10^{-3}	2.0299	1.0214
80	Mesh 32	3.3786×10^{-3}	2.0098	1.0071
160	Mesh 64	1.6903×10^{-3}	1.9988	0.9991

Table 5
Requirements and penalty amounts for each energy year.

Energy year	2011	2012	2013
Requirement (R_i)	306 000	442 000	596 000
Penalty (π_i)	675	658	641

In both cases, the computed errors and the convergence ratio shown in Tables 3 and 4 illustrate first order convergence. Moreover, the qualitative results for both cases are very close. Nevertheless, the errors are a bit lower when the characteristics curves can be computed analytically.

In [4], the same nonlinear PDE is solved by replacing the Lagrange–Galerkin method by a finite differences schemes and first order convergence is also met. However, more refined meshes are necessary in [4] to obtain similar errors, which involves larger computing time.

Concerning the fixed-point algorithm explained in Section 4.4, the convergence is attained in one or few iterations for the same tolerance as in [4]. Moreover, we have empirically checked that the relative errors are not too much influenced by this tolerance, although the computational cost is highly increased. Furthermore, the choice of the parameter ω was carried out empirically.

Although second order convergence could be expected for the here treated nonlinear problem, the authors understand that the main reason for the observed first order convergence is due to the nonlinear aspect of the problem. Also, first order convergence has been observed for separate refinements of the time and spatial meshes.

Finally, note that for the analytical tests developed in [16], a second-order convergence is obtained with respect to time and space. However, we point out that the academic tests in [16] were developed for a linear PDE problem and under certain assumptions on the velocity field.

5.2. Real case: pricing of a green certificate

In order to show an example of the pricing of a real REC, we consider the numerical solution of problem (12) with real data taken from the literature. As in [4], we use some from the New Jersey market data for Solar Renewable Energy Certificates (SRECs) presented in [5]. In this setting, we carry out the valuation of a SREC with maturity $T = 13$, which corresponds to the end of energy year 2013, which is May 31, 2013, as it is indicated in [5]. Moreover, we assume that energy year 2013 matches the time interval $(12, 13]$. Additionally, we consider that the certificate has 3 years of life, i.e. $y = 3$. Hence, the beginning of the certificate is $t = T - y = 10$ (or equivalently $\tau = y = 3$), which is the end of energy year 2010, and the first compliance date is $t = 11$ (i.e. end of energy year 2011) which corresponds to $\tau = 2$.

For this certificate, in Table 5 we show the values of the requirements at the end of each energy year and the corresponding penalties if the requirements are not met. Note that the end of each energy year corresponds to maturity or compliance date. At these dates, either the payoff or the appropriate jump conditions are applied. Additionally, the values of the parameters γ_g, δ_g, σ_g and r are the same as the ones included in Table 2 for the analytical test. In this real case, the valuation of the certificate is performed when seasonal effects are taken into account and modelled with the function given by (25).

Regarding the parameters involved in the numerical methods, we have chosen $\bar{G}_\infty = 2 \times \ln(8 \times 10^5)$ and $B_\infty = 8 \times 10^3$. Moreover, in order to solve the real case, we have employed Mesh 16, the data of which are reflected in Table 1, while

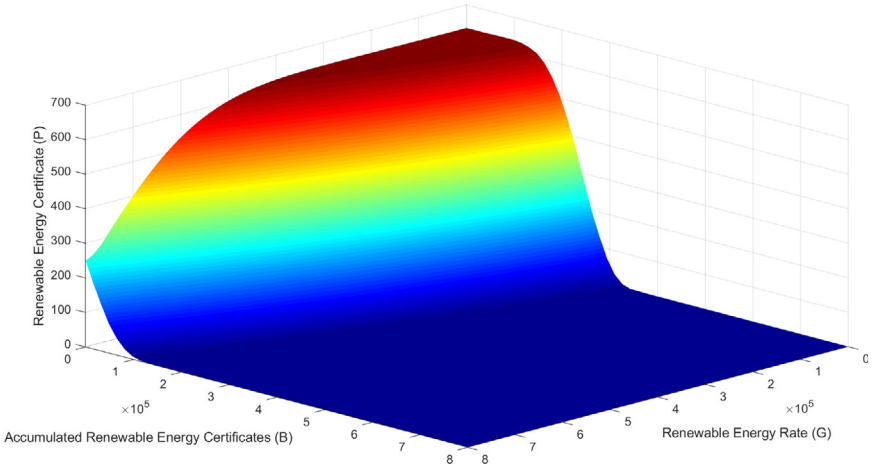

Fig. 1. Renewable energy certificate price at time $t = T - 2/3$.

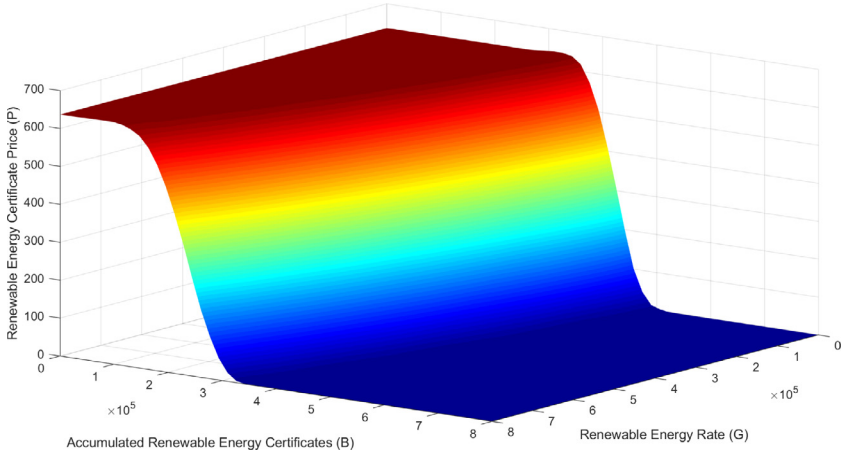

Fig. 2. Renewable energy certificate price at time $t = T - 1/3$.

for the time discretization we have considered 100 time steps per month, i.e. $\Delta\tau = \frac{1}{1200}$. Finally, the parameter (ω) in the duality method is set to 2×10^{-5} and the tolerance ϵ is equal to 10^{-5}, which is again achieved in one or few iterations.

As in [4], in Fig. 1 we show the price of the certificate eight months before maturity, that is at time $t = T - 2/3$ (or $y = 2/3$, equivalently), taking values between zero and the penalty amount, π. On the one hand, we can observe that when the values of accumulated supply, B, and renewable energy, $G = \exp(\tilde{G})$, are low, the price of the certificate tends to the penalty value. On the other hand, when the value of both state variables increases, the price of the certificate decreases, as in [5]. More precisely, for high values of B, the price goes very low, and vice versa. Nevertheless, when high values of G do not offset low values of B, the price goes towards the penalty, as it is shown in Fig. 1.

Next, in Fig. 2 we represent the value of the certificate for a time closer to maturity, actually four months before maturity, i.e., at time $t = T - 1/3$. At this time, we can observe that, for values of accumulated certificates nearer to requirement, low values of generation rate are linked to certificate prices equal to the penalty amount. Additionally, for lower values of banked certificates, high enough values of generate rate are associated with prices equal to the penalty. As expected, a low number of accumulated renewable energy certificates is compensated by a high production of renewable energy.

Finally, for large enough values of renewable energy rate, in Fig. 3 we represent the price of the certificate versus the number of accumulated renewable energy certificates for different times, obtaining some cross-sectional plots similar to the ones in [4]. At $t = T$, which coincides with maturity, the REC price matches the penalty if the requirement is not met, otherwise the price is zero. Then, as we move backwards in time, the curves take lower values and move to the left, due to the diffusion of the final value. This behaviour can be also observed in [4,5]. Moreover, due to the jump condition imposed at compliance dates, an increment in the price and a jump to the right appears when arriving at this date. Thus, in Fig. 3 we show the value at the first compliance date as well. As it is pointed out in [5] and also observed in [4], at maturity

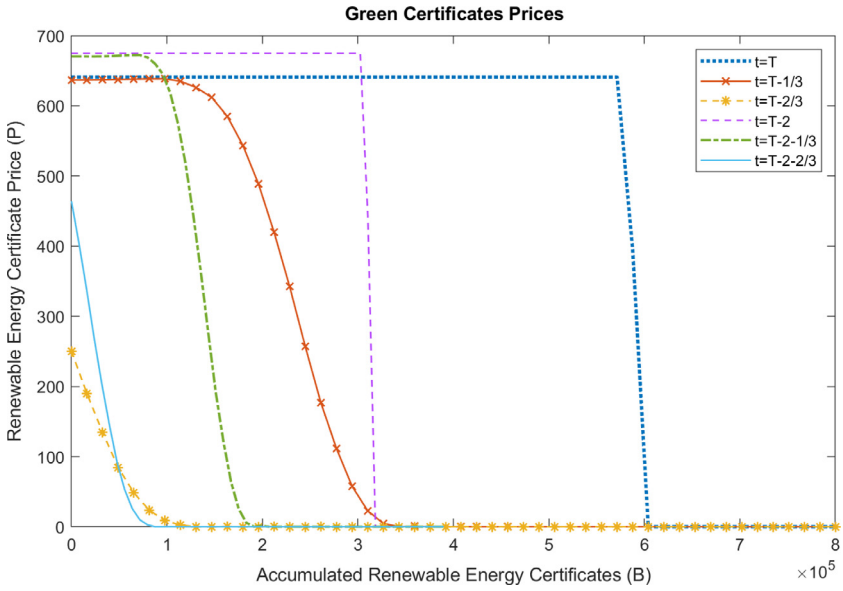

Fig. 3. Price curves for different times.

Table 6
Convergence order at time $t = T - 2/3$ for the mesh point $(G, B) = (100\,000, 200\,000)$ in the real case.

Time steps	Meshes	REC value (P)	R	Order
80	Mesh 4	186.6418	–	–
160	Mesh 8	310.8065	–	–
320	Mesh 16	427.2542	1.0662	0.0926
640	Mesh 32	485.6351	1.9946	0.9961
1280	Mesh 64	503.9941	3.1799	1.6691

and compliance dates there exists a discontinuity when the number of accumulated certificates meets the requirement, because of the penalization multiplied by the indicator function.

The CPU time is 123 s for this real case example, i.e., this method is faster than the first one presented in [4] which requires 223 s. The CPU of the laptop we use is an Intel(R) Core(TM) i7-10750H at 2,6 GHz with 32 GB 2933 MHz DDR4 RAM.

In this real case, we have also checked the experimental order of convergence. As the analytical solution is not available, we compute the indicator of convergence order, R, at a given mesh point, which is given by

$$R = \frac{P\left(\frac{\tilde{h}}{2}\right) - P(\tilde{h})}{P\left(\frac{\tilde{h}}{4}\right) - P\left(\frac{\tilde{h}}{2}\right)},$$

where P is the REC price at the given point and the parameter $\tilde{h}$ indicates that we start with a level of refinement in time and space and divide by two both the time and finite element mesh steps to get the results for $\frac{\tilde{h}}{2}$. Finally, the order of convergence is given by $\log_2(R)$. Thus, $R = 2$ corresponds to first order convergence while $R = 4$ corresponds to second order convergence. Tables 6 and 7 show the pointwise error and order of convergence at time $T = t - 2/3$ at two different values, after computing the value of the REC at each particular point as well as the value of the error indicator R. Note that the computed of order of convergence for the two points is between one and two. As shown in the tables we have chosen two points are mesh nodes for all considered meshes and for which the value of the REC is greater than zero and less than the penalization value.

6. Conclusions

The number of financial institutions interested in trading energy and power derivatives is growing and it has sparked a drive in both industry and academia to find suitable mathematical models. The objective of this paper has been the numerical solution of pricing problems related to renewable energy certificates (RECs) or green certificates. For this purpose, we propose appropriate numerical methods different to the ones applied to this problem before.

Table 7
Convergence order at time $t = T - 2/3$ for the mesh point $(G, B) = (400\,000, 100\,000)$ in the real case.

Time steps	Meshes	REC value (P)	R	Order
80	Mesh 4	313.5751	–	–
160	Mesh 8	449.3907	–	–
320	Mesh 16	514.4062	2.0889	1.0628
640	Mesh 32	545.1797	2.1127	1.0791
1280	Mesh 64	555.7902	2.9003	1.5362

In particular, we characterize the green certificate price as the solution of a degenerate PDE with a nonlinear convective term due to the dependence of the drift on the unknown of the problem. Concerning this issue, an appropriate maximal monotone operator is introduced to formulate the nonlinear problem. In this way, the nonlinear convection term can be treated by means of a duality algorithm proposed by Bermúdez and Moreno. At each time step of the fixed point algorithm, the linear problem is discretized by means of a characteristics Crank–Nicolson Lagrange–Galerkin method, which is the main contribution of this paper.

Numerical results obtained in an academic problem with analytical solution, that has been used as sanity check, illustrate the performance of the method. Next, the consideration of a real REC pricing problem is addressed (taken from the SREC markets) and reasonable results are obtained which can be compared with the ones in [4]. In terms of computational time, the proposed method outperforms the one proposed in [4].

Future research will focus on the mathematical modelling and numerical solution for the pricing of financial derivatives of RECs, that are increasingly traded in energy markets.

Data availability

No data was used for the research described in the article.

Acknowledgements

The authors acknowledge the funding by Spanish MINECO with the grants MTM2016-76497-R and PID2019-10858RB-I00, and by Galician Government, Spain with the grants ED431C 2018/033 and ED431C 2022/47, both including FEDER financial support. As members of CITIC, they also acknowledge the grant ED431G 2019/01, funded by Consellería de Educación, Universidade e Formación Profesional of Xunta de Galicia through FEDER funds with 80%, from FEDER Galicia 2014–2020 Program and 20% from Secretaría Xeral de Universidades.

References

[1] S. Howison, D. Schwarz, Risk-neutral pricing of financial instruments in emission markets: A structural approach, SIAM Rev. 57 (2015) 95–127.
[2] J. Seifert, M. Uhrig-Homburg, M. Wagner, Dynamic behavior of CO_2 spot prices, J. Environ. Econ. Manag. 56 (2008) 180–194.
[3] T. Tietenberg, Environmental and Natural Resource Economics, sixth ed., Munich et al.: Addison Wesley, Boston, 2003.
[4] M.A. Baamonde-Seoane, M.C. Calvo-Garrido, M. Coulon, C. Vázquez, Numerical solution of a nonlinear PDE model for pricing renewable energy certificates (RECs), Appl. Math. Comput. 404 (2021) 126199.
[5] M. Coulon, J. Khazaei, W.B. Powell, SMART-SREC: A stochastic model of the New Jersey solar renewable energy certificate market, J. Environ. Econ. Manag. 73 (2015) 13–31.
[6] A. Shrivats, S. Jaimungal, Optimal generation and trading in solar renewable energy certificate (SREC) markets, Appl. Math. Finance 27 (1–2) (2020) 99–131.
[7] K.M. Currier, A regulatory adjustment process for the determination of the optimal percentage requirement in an electricity market with Tradable Green Certificates, Energy Policy 62 (2013) 1053–1057.
[8] A. Verbruggen, Tradable Green Certificates in Flanders (Belgium), Energy Policy 32 (2) (2004) 165–176.
[9] F. Dong, L. Shi, X. Ding, Y. Li, Y. Shi, Study on China's renewable energy policy reform and improved design of renewable portfolio standard, Energies 12 (11) (2019) 2147.
[10] X. Ye, Z. Li, C. Wang, X. Lei, W. Yuan, Z. Shi, Green power certificates in China: A study on pricing and transaction decisions, in: Chinese Automation Congress (CAC), Hangzhou, China, 2019, pp. 5605–5608.
[11] F.E. Benth, M. Eriksson, S. Westgaard, Optimal management of green certificates in the Swedish-Norwegian market, J. Energy Mark. 10 (2017) 1–39.
[12] M. Ghaffari, A. Hafezalkotob, A. Makui, Analysis of implementation of Tradable Green Certificates system in a competitive electricity market: A game theory approach, J. Ind. Eng. Int. 12 (2016) 185–197.
[13] A. Bermúdez, C. Moreno, Duality methods for solving variational inequalities, Comput. Math. Appl. 7 (1981) 43–58.
[14] A. Bermúdez, M.R. Nogueiras, C. Vázquez, Numerical solution of variational inequalities for pricing Asian options by higher order Lagrange-Garlerkin methods, Appl. Numer. Math. 56 (2006) 1270–1526.
[15] A. Bermúdez, M.R. Nogueiras, C. Vázquez, Numerical analysis of convection–diffusion-reaction problems with higher order characteristics finite elements. Part I: Time discretization, SIAM J. Numer. Anal. 44 (2006) 1829–1853.
[16] A. Bermúdez, M.R. Nogueiras, C. Vázquez, Numerical analysis of convection–diffusion-reaction problems with higher order characteristics finite elements, Part II: Fully discretized scheme and quadrature formulas, SIAM J. Numer. Anal. 44 (2006) 1854–1876.
[17] J.J. Lucia, E.S. Schwartz, Electricity prices and power derivatives: Evidence from the nordic power exchange, Rev. Deriv. Res. 5 (2002) 5–50.

[18] M.C. Calvo-Garrido, M. Ehrhardt, C. Vázquez, Pricing swing options in electricity markets with two stochastic factors using a partial differential equation approach, J. Comput. Finance 20 (2017) 81–107.
[19] K. Itô, On stochastic differential equations, Mem. Amer. Math. Soc. 4 (1951) 1–51.
[20] D. Schwartz, Price Modelling and Asset Valuation in Carbon Emission and Electricity Markets, (Ph.D. thesis), University of Oxford, Oxford, UK, 2012.
[21] J. Ma, Z. Wu, D. Zhang, J. Zhang, On well-posedness of forward–backward SDEs — A unified approach, Ann. Appl. Probab. 25 (4) (2015) 2168–2214.
[22] J. Ma, H. Yin, J. Zhang, On Non-Markovian Forward–Backward SDEs and Backward Stochastic PDEs, Working paper, 2012.
[23] J. Ma, J. Yong, Forward-Backward Stochastic Differential Equations and their Applications, Springer, 1999.
[24] I. Arregui, J.J. Cendán, C. Vázquez, A duality method for the compressible Reynolds equation, application to simulation of read/write processes in magnetic storage devices, Int. J. Comput. Appl. Math. 175 (2005) 31–40.
[25] I. Arregui, J.J. Cendán, C. Parés, C. Vázquez, Numerical simulation of a 1-D elastohydrodynamic problem in magnetic storage devices, ESAIM Math. Model. Numer. Anal. 42 (2008) 645–665.
[26] I. Arregui, J.J. Cendán, C. Vázquez, Adaptative numerical methods for an hydrodynamic problem arising in magnetic reading devices, Math. Comput. Simulation 99 (2014) 190–202.
[27] H. Brézis, Analyse Fonctionelle, Masson, Paris, 1983.
[28] O.A. Oleinik, E.V. Radkevic, Second Order Equations with Nonnegative Characteristic Form, American Mathematical Society, Providence, Rhode Island, Plenum Press, New York-London, 1973.
[29] M.R. Nogueiras, Numerical Analysis of Second Order Lagrange-Galerkin Schemes. Application to Option Pricing Problems, (Ph.D. thesis), University of Santiago de Compostela, 2005.